Effects of toceranib compared with sorafenib on monocrotaline-induced pulmonary arterial hypertension and cardiopulmonary remodeling in rats

Zi Ping Leong[a], Yoshiaki Hikasa[a,b*]

[a]The United Graduate School of Veterinary Science, Yamaguchi University, 1677-1, Yoshida, Yamaguchi 753-8515, Japan

[b]Joint Department of Veterinary Medicine, Laboratory of Veterinary Internal Medicine, Faculty of Agriculture, Tottori University, Tottori 680-8550, Japan

*Corresponding author. E-mail address: hikasa@muses.tottori-u.ac.jp (Y. Hikasa); Mailing address: Joint Department of Veterinary Medicine, Laboratory of Veterinary Internal Medicine, Faculty of Agriculture, Tottori University, Tottori 680-8550, Japan

Abstract

Sorafenib reverses pulmonary arterial hypertension (PAH) and cardiopulmonary remodeling (CPR), but the effects of toceranib are unknown. This study investigated anti-remodeling effects and determined optimal doses of toceranib and sorafenib on monocrotaline (MCT)-induced PAH and CPR in rats. MCT-treated rats were orally treated with a 14-day course of sorafenib (10, 30, or 100 mg/kg), toceranib (1, 3, or 10 mg/kg), or water. Both sorafenib and toceranib significantly reversed the right ventricular (RV) hypertrophy at 10 mg/kg, but only sorafenib significantly improved the RV systolic and mean pressures. Sorafenib significantly normalized the B-type natriuretic peptide mRNA level of the RV and increased the non-muscularized pulmonary artery percentage. However, these effects were only observed at the highest toceranib dose, and neither toceranib dose reduced the fully muscularized pulmonary artery percentage. Further, the inhibition on vascular endothelial growth factor (VEGF) signaling was stronger in sorafenib than in toceranib. Besides the stronger inhibition on mitogen-activated protein kinase signaling, the greater reversal ability of sorafenib may be also due to the simultaneous blockade on the C-X-C chemokine receptor type 4 and autophagy induction. Toceranib insignificantly reversed CPR, and a high-dose therapy did not improve the RV hemodynamic outcomes. Sorafenib significantly reversed CPR, and a low-dose sorafenib therapy may be a suitable therapeutic agent for PAH.

Keywords: Cardiopulmonary remodeling, pulmonary arterial hypertension, right ventricular hypertrophy, sorafenib, toceranib

1. Introduction

Pulmonary arterial hypertension (PAH) is characterized by proliferation of pulmonary arterial smooth muscle cells and right ventricular hypertrophy (RVH), and remains an incurable disease with a poor long-term prognosis [5,29]. After the discovery of an increased downstream mitogen-activated protein kinase (MAPK) signaling from the receptor TKs in the PAH pathogenesis, many studies have investigated the reversal effects of tyrosine kinase (TK) inhibitors, such as imatinib [8,11,34], sunitinib [17], and sorafenib [16,30] on experimental and clinical PAH. However, most of the studies evaluated the effects of high doses of the TK inhibitors, and only a few examined those of low doses [2,10,20]. Nonetheless, we recently showed that low-dose imatinib significantly reversed monocrotaline (MCT)-induced RVH and pulmonary remodeling in rats [20] and improved hemodynamics in dogs with PAH [2].

In the continuous search for a TK inhibitor which possesses potent properties against cardiopulmonary remodeling (CPR) to allow administration at a lower, non-neoplastic dose and avoid adverse effects, we investigated toceranib (SU11654), a veterinary TK inhibitor approved for the therapy of canine mast cell tumors. Several studies of canine malignancies have shown that toceranib acts via the inhibition of mutated c-KIT receptors and angiogenesis [18,24,25]. However, no single study has reported its efficacy in reversing the PAH nor CPR. The structural and functional similarities of toceranib and sunitinib [25] provide a compelling rationale for investigating whether toceranib reverses PAH and CPR or otherwise aggravates angioproliferation via vascular endothelial growth factor (VEGF) signaling inhibition as reported in our recent study [20].

Sorafenib, a multi-kinase inhibitor, shows favorable hemodynamic effects in patients with refractory PAH [14], and potent anti-remodeling effects against RVH and pulmonary

muscularization in rats treated with MCT or hypoxia [16,30]. Therefore, we compared the reversal effects of toceranib with sorafenib on MCT-induced PAH and CPR in rats. The present study also improved the shortcoming of our previous study by scrutinizing effects of both agents on the right ventricular hemodynamics, and determined the optimal dose of each agent for the treatment of severe PAH. Besides, sorafenib has also been reported to induce apoptosis and affects autophagy in myeloid dendritic cells [21], human macrophages [22], and hepatic carcinoma cells [40], thus raising the possibility that it may also confer a beneficial effect by improving the impaired autophagy in the PAH lungs [12,26]. Because both sorafenib and toceranib act on the PDGF and c-KIT receptors, in which their expression and accumulation are in turn influenced by the C-X-C motif chemokine ligand 12/ C-X-C motif chemokine receptor 4 (CXCL12/CXCR4) pathway [40], we also investigated the unclear role of the CXCL12/CXCR4 axis in the MCT-induced PAH.

2. Materials and methods

2.1. Monocrotaline-induced pulmonary arterial hypertension and treatments

All experimental procedures were approved by the Institutional Animal Care and Use Committee of the Tottori University and carried out as described previously [20] with some modifications. Male Wistar-Imamichi rats were randomized into three groups: the placebo and treatment groups received a single subcutaneous injection of 60 mg/kg of MCT (Sigma-Aldrich, China), whereas the control group received physiological saline. On day 14 after the injection, the treatment rats were medicated with either sorafenib [Nexavar 200 mg, Bayer: 10 (sora-10), 30 (sora-30), or 100 (sora-100) mg/kg per day] or toceranib phosphate [Palladia 50 mg, Pfizer: 1 (toce-1), 3 (toce-3), or 10 (toce-10) mg/kg per day]. The control and placebo rats were given water. All the treatments were

administered orally, once daily for 14 days.

2.2. Measurement of RV hemodynamic parameters

The rats were anesthetized with 2% isoflurane via a face mask. A polyethene catheter (PE-50 Intramedic PE tubing, Becton Dickinson) was advanced into the RV via the right jugular vein to measure RV systolic pressure (RVSP), mean RV pressure (RVP) and heart rate (HR). The position of the catheter was confirmed by the pressure waveforms. The data were recorded and analyzed with the PowerLab System connected a pressure transducer (ADInstruments), after which the rats were euthanized for tissue sampling.

2.3. Assessment of RVH

The RV tissue was dissected from the left ventricle and septum (LV+S). Wet weights of the RV and LV+S were determined to derive the RVH index: [RV/(LV+S)].

2.4. Histology of pulmonary arterial muscularization

Left lung lobes were subjected for histological preparation and elastic van Gieson (EVG) staining. The proportions of pulmonary arteries of 20–50 μm in diameter that were fully muscularized (FMPA), partially muscularized (PMPA), and non-muscularized (NMPA) were determined as described previously [20]. In addition, we also measured the external diameter (d), medial wall thickness (MWT), MWT ratio ($2\times MWT/d\times 100\%$), lumen diameter ($d-2\times MWT$), and lumen area [$3.142\times(d/2)^2$] of FMPAs that were 20–50 μm and 51–100 μm in diameter using Image J software.

2.5. Semi-quantitative fast real-time polymerase chain reaction

First-strand complementary DNA was synthesized from 2 μg RNA, which was isolated from the RV tissue and the right caudal lung lobes, respectively, using the Superscript® III First-Strand Synthesis System (Invitrogen, USA). In addition to the previously described target messenger RNAs (mRNAs) [20], p-62 (forward:

CCTGAAGAATGTGGGGGAGAG; reverse: TGTGCCTGTGCTGGAACTTT), KIT proto-oncogene receptor TK (c-KIT) (forward: GGCAAATACACGTGCGTCAG; reverse: AAACAAGGGAAGGCCAACCA), C-X-C motif chemokine (CXC) receptor 4 (CXCR4) (forward: CCGTCTATGTGGGTGTCTGG; reverse: CACAGATGTACCTGCCGTCC), and CXC ligand 12 (CXCL12) (forward: CACTCCAAACTGTGCCCTTC; reverse: CGGGTCAATGCACACTTGTCT) expression levels were also determined with Applied Biosystems 7500 Fast Real-Time PCR System using SYBR® Fast qPCR Mix (Takara Bio Inc., Shiga, Japan).

2.6. Western blotting assay

Lysates of lung tissues were separated on 4–15% sodium dodecyl sulfate-polyacrylamide gels (Mini-PROTEAN® TGX™ Precast Protein Gels, Bio-Rad, USA) and transferred to polyvinylidene difluoride membranes. The membranes were blocked with Tris-buffered saline (EzTBS, Atto, Japan) containing 1% bovine serum albumin for 1 hour at room temperature, and incubated with one of the following primary antibodies: anti-phospho-extracellular-signal-related kinase (ERK) 1/2 (Cell Signaling Technology, Inc., USA), anti-ERK 1/2 (Santa Cruz Biotechnology Inc., Santa Cruz, CA, USA), anti-VEGF-A, anti-VEGF receptor (VEGFR) 2, anti-microtubule-associated protein 1 light chain (LC) 3B (Abcam, Cambridge, UK), or anti-β-actin (Santa Cruz Biotechnology Inc., Santa Cruz, CA, USA). Then, we performed a subsequent incubation using a specific secondary antibody conjugated to horseradish peroxidase. Bio-Rad Universal Hood II and Image Lab Software 6.0 (Bio-Rad Laboratories) were used to visualize and quantify the chemiluminescence, respectively.

2.7. Statistical analyses

All data are expressed as means±standard error of the mean (SEM) and tested for

significance using one-way analysis of variance and Tukey's post-hoc test for inter-group differences. Non-normally distributed data were analyzed using the Mann–Whitney U test to determine the differences between two independent groups. The relationship between treatment effects and dosages was analyzed using simple linear regression and the Pearson correlation test. Significance was set at $P<0.05$.

3. Results

3.1. RV hemodynamic parameters and HR

The control rats had RVSP of 24.05±1.00 mmHg and mean RVP of 5.88±0.77 mmHg, whereas rats in the placebo group had higher RVSP and mean RVP of 70.46±2.00 mmHg and 25.03±1.47 mmHg, respectively (Fig. 1A). Compared with placebo, the rats in sora-10 group had significantly lower RVSP (52.07±6.67 mmHg), mean RVP (17.48±1.84 mmHg), and HR (246.06±15.39 bpm). By contrast, toce-10 did not significantly decrease the RVSP (69.65±8.44 mmHg) nor mean RVP (22.20±3.29 mmHg).

3.2. RV remodeling

Compared with the placebo (0.55±0.03), sora-10 (0.38±0.03), sora-30 (0.37±0.04), and sora-100 (0.29±0.03) significantly and dose-dependently (R^2=0.35, $P<0.05$) reversed RVH (Fig. 1B). In the toceranib groups, a significant RVH reversal was observed only in the toce-10 (0.34±0.04) group. Further, BNP mRNA expression as a RVH marker also exhibited a similar trend (Fig. 1C). Compared with the placebo with the highest BNP mRNA expression (0.53±0.03), all doses of sorafenib, and toce-10 (0.26±0.06) significantly and dose-dependently ($_{sorafenib}R^2$:0.38, $_{toceranib}R^2$:0.27, $P<0.05$) downregulated the BNP mRNA expression.

3.3. Muscularization of 20–50 μm pulmonary arteries

Representative photomicrographs of NMPAs, PMPAs, and FMPAs are shown in Fig.

2A. The proportion of FMPAs in the placebo (43.13±2.41%) was significantly increased after the MCT injection (Fig. 2B) to indicate an occurrence of pulmonary remodeling. Compared with the placebo, only the sora-100 group showed significant FMPA reduction (29.71±2.14%), although treatments with sora-10 (39.88±2.70%) and sora-30 (38.07±1.88%) insignificantly reduced the proportion of FMPAs. In the toceranib groups, neither dose significantly decreased the proportion of FMPAs. Furthermore, dose-dependent FMPA reduction was stronger in sorafenib (R^2=0.33, P<0.05) than in toceranib (R^2=0.01) (Fig. 2C). Besides, the proportion of NMPAs was significantly increased in all sorafenib groups and the toce-10 group (17.18±1.02%). In this aspect, sorafenib and toceranib produced R^2 values of 0.51 and 0.34 (P<0.05), respectively (Fig. 2D). The proportion of PMPAs was significantly higher in the placebo (50.62±2.75%) but did not differ significantly between the treatment and control groups.

3.4. Medial hypertrophy and lumen area of 20–50 μm FMPAs

In the placebo group, proliferation of smooth muscle cells increased the MWT ratio (49.91±1.41%) and reduced the lumen area (224.03±9.35 μm^2) of the 20–50 μm FMPAs (Fig. 3A,B). These values differed significantly from those in the control (MWT ratio=34.38±1.19%, lumen area=399.15±15.52 μm^2). In the treatment groups, all doses of sorafenib significantly reversed the medial hypertrophy and increased the lumen area. Although all doses of toceranib produced a significant MWT reduction, the increase in lumen area was significant only in the toce-10 group (293.66±10.97 μm^2).

3.5. Medial hypertrophy and lumen area of 51–100 μm FMPAs

The 51–100 μm FMPAs of the placebo group also noticeably increased MWT ratios (54.73±1.95%) and decreased lumen areas (842.64±53.97 μm^2) (Fig. 3C,D). Both sorafenib and toceranib significantly reversed the MWT ratio and increased the lumen

area of the FMPAs.

3.6. PDGFR-β, C-KIT, CXCR4, CXCL12 and nestin mRNA expression in the lungs

The pathogenic role of PDGFR-β in MCT-induced pulmonary remodeling was shown by a significant, 3-fold mRNA upregulation in the placebo (0.090±0.019) compared with that in the control (0.029±0.004) (Fig. 4A). Except for the toce-1 group (0.048±0.008), all treatment groups significantly normalized the mRNA expression to a level comparable with that of the control. Besides, the c-KIT mRNA level was higher in the placebo (0.038±0.007) than that in the control (0.028±0.005), although insignificantly (Fig. 4B). In the treatment groups, it was significantly decreased by sora-10 (0.019±0.003), sora-30 (0.017±0,005), toce-3 (0.018±0.005) and toce-10 (0.019±0.003) compared with the placebo, indicating an inhibitory property against c-KIT by both TK inhibitors. The MCT treatment also upregulated the mRNA levels of the stem cell mobilizers: a 2-fold increase in CXCR4 (0.179±0.044; P=0.196) and a 3-fold increase in CXCL12 (0.241±0.043; P<0.05) (Fig. 4C), compared with that in the control (CXCR4: 0.088±0.008; CXCL12: 0.070±0.010). In the treatment groups, only sorafenib (sora-10: 0.075±0.016; sora-30: 0.054±0.007 and sora-100: 0.054±0.005) significantly downregulated the CXCR4 mRNA. However, neither sorafenib nor toceranib significantly suppressed the CXCL12 mRNA levels, although both tended to reduce it. Further, the nestin mRNA levels did not vary significantly among the control (0.023±0.002), placebo (0.023±0.004), and treatment groups (Fig. 5D). However, compared with the placebo group, the toce-1 group insignificantly upregulated the mRNA level (0.031±0.007).

3.7. VEGF signaling pathway in the lungs

Since sorafenib and toceranib are VEGFR inhibitors, we studied their inhibitory

effects on mRNA and protein levels of VEGFR-2 (Fig. 5A,B) and VEGF-A (Fig. 5B,C) in the lungs. The MCT administration did not increase levels of VEGFR-2 mRNA (0.272±0.024) and protein (0.41±0.07), nor VEGF-A mRNA (0.052±0.008) and protein (0.138±0.004) levels. The VEGFR-2 protein expression also did not remarkably differ among the treatment groups, although the sora-100 group showed a significant lower mRNA level (0.182±0.026) than the placebo. With respect to the VEGF-A levels, sora-30 (mRNA=0.024±0.004, protein=0.121±0.001) and sora-100 (mRNA=0.029±0.004, protein=0.117±0.006) significantly suppressed the mRNA and protein levels. Although the mRNA levels were significantly reduced in the toce-3 (0.022±0.004) and toce-10 (0.021±0.022) groups, a significant protein reduction was observed only in the toce-10 group (0.155±0.002) compared with the placebo.

3.8. MAPK signaling pathway in the lung

We investigated Raf-1 mRNA (Fig. 6A) and phosphorylated ERK-1/2 protein (Fig. 6B,C) expression, which constitute the MAPK signaling pathway. Compared with the control (0.066±0.010), the placebo noticeably elevated the Raf-1 mRNA expression (0.150±0.020). Downregulation of the mRNA was significant in the sora-30 (0.082±0.012), sora-100 (0.058±0.008), and toce-10 (0.097±0.011) groups. Further, the dose-dependent Raf-1 inhibition of sorafenib (R^2=0.27, $P<0.05$) was stronger than that of toceranib (R^2=0.10) (Fig. 6A). Phosphorylation of the ERK-1/2 protein was markedly upregulated in the placebo (2.82±0.13) compared with the control (0.44±0.17). In comparison with the placebo, all doses of sorafenib, but only toce-10 (1.42±0.29) for the toceranib groups, significantly inhibited the ERK-1/2 phosphorylation. Notably, rats that received the lowest sorafenib dose (1.43±0.36) had a phosphorylated protein level that is comparable with that received the highest toceranib dose, suggesting an equal inhibitory

strength on the MAPK pathway by sorafenib and toceranib at a dose of 10 mg/kg.

3.9. Autophagy markers in the lungs

Because LC3-1 detection is affected by many factors and LC3-II/LC3-I ratio is an unreliable indicator for autophagy [38], we compared the amount of LC3-II with β-actin. The LC3-II/β-actin protein level did not differ significantly between the control (0.34±0.06) and placebo (0.37±0.06) groups (Fig. 7A). Compared with the placebo, sora-10 (0.44±0.04) and sora-30 (0.40±0.07) tended to increase the protein level, whereas toce-3 (0.32±0.05) and toce-10 (0.24±0.04) tended to suppress the protein level. As for the p-62 mRNA levels, the control (0.217±0.029), placebo (0.208±0.030), toce-3 (0.254±0.025), and toce-10 (0.249±0.032) groups showed comparable levels (Fig. 7B). By contrast, sora-10 (0.324±0.064; $P=0.06$) and sora-30 (0.362±0.055; $P<0.05$) upregulated the mRNA levels, indicating a higher autophagy level in the rat lungs. Besides, sorafenib also produced a higher dose-dependency ($R^2=0.15$, $P<0.05$) than toceranib ($R^2=0.02$).

4. Discussion

This study is the first to demonstrate the reversal effects of toceranib on MCT-induced pulmonary arterial hypertension and cardiopulmonary remodeling in rats. Our results show that treatment with a high dose of toceranib (10 mg/kg) led to only a partial inhibition of pulmonary muscularization without improving the RV hemodynamic outcomes, whereas treatment with low doses (1 and 3 mg/kg) yielded insignificant anti-remodeling effects on RV and pulmonary muscularization. Besides, we also confirm the potent cardiopulmonary reversal effects of sorafenib. A low-dose sorafenib therapy (10 mg/kg) significantly improved PAH not only via a potent inhibition on the MAPK but also the CXCL12/CXCR4 signaling pathways, as well as an autophagy induction in the lungs.

Toceranib phosphate is a veterinary TK inhibitor licensed for the treatment of canine mast cell tumors. In terms of kinase selectivity, toceranib targets PDGFR-β, VEGFR-2, and c-KIT receptors and has cellular half-maximal inhibitory concentrations of 0.01–0.1, 0.005–0.05, and 0.01–0.1 μM, respectively [23]. Sorafenib has a wider activity spectrum that inhibits not only c-KIT, VEGFR-2, and PDGFR-β but also serine/threonine kinase Raf-1 [15]. Consistently, rats that received any dose of sorafenib, and 3 or 10 mg/kg of toceranib had lower PDGFR-β and c-KIT mRNA levels. Notably, the PDGFR-β mRNA downregulation by toceranib was weaker than sorafenib. Expectedly, the Raf-1 inhibiting sorafenib resulted in a greater inhibition on the Raf-1 mRNA than toceranib.

In beagle dogs receiving a 14-day course of an anti-neoplastic toceranib dose (3.25 mg/kg, orally, every other day), it achieved elimination half-life ($T_{1/2}$) of 17.2±3.9 hours, time to maximum plasma concentration (Tmax) of 6.2±2.6 hours, and area under the plasma concentration time-curve (AUC_{0-48}) of 2640±940 ng·h/ml [37]. By contrast, the 14-day therapy with a low-dose sorafenib (100 mg, orally, twice daily) in the Japanese patients yielded mean $T_{1/2}$ of 27.1 hours, Tmax of 4 hours, and AUC_{0-12} of 9400 ng·h/ml [28]. The pharmacokinetic differences imply that a further increment in the toceranib dose may augment the reversal potency by optimizing the drug exposure to a level that is comparable to that of sorafenib. However, the full-blown toxicity and side effects associated with the dose escalation may raise a safety concern.

With respect to pulmonary arterial remodeling, we showed that sorafenib dose-dependently reversed muscularization by increasing the proportion of NMPAs. This reversal achieved a statistical significance even in rats that received the lowest dose (10 mg/kg) and confirmed the results by Klein et al. [16]. However, a high dose (10 mg/kg) of toceranib was required to produce a significant increase in NMPAs. In addition, low,

medium, and high doses of sorafenib dose-dependently reduced the proportion of FMPAs by 7.5%, 11.7%, and 31.1%, respectively. Conversely, in the toceranib groups, the high dose normalized the FMPAs by 1.4%, whereas the low dose caused an additional increase of 12%. The above findings may explain the reason of an insignificant reduction in RVSP and mean RVP in the rats at the highest dose of toceranib. Further, the increase in the lumen area of the 20–50 μm FMPAs and the insignificant ERK 1/2 de-phosphorylation in the toce-1 and toce-3 groups also indicate that toceranib has a weak reversal effect on pulmonary remodeling when administered at lower doses.

Moreno-Vinasco et al. [30] showed that sorafenib administered at a dose of 2.5 mg/kg significantly reversed RVH and pulmonary arterial muscularization, and improved RV systolic pressure in rats subjected to hypoxia alone or combined hypoxia and SU5416 treatments. However, rats in the placebo had a RVH index of approximately 0.4 and a mean RVSP of less than 30 mmHg, which collectively indicated a mild PAH. In the present study, we documented a greater RVSP (70.46±2.00 mmHg) and a higher RVH index (0.55±0.03) in the placebo rats, indicating that a severe PAH occurred 28 days after the MCT administration. This finding also agreed with the results of studies by Schermuly et al. [34] and Klein et al. [16], which reported RVH indexes of 0.71±0.03 (RVSP>60 mmHg) and 0.51±0.02 (RVSP=82.9±6.0 mmHg), respectively. Therefore, we believe that the dose of 2.5 mg/kg may be too low for effective cardiopulmonary reversal, at least for the MCT-induced severe PAH model.

We previously showed that potent VEGF signaling inhibition by sunitinib elevated nestin mRNA levels, exacerbated vascular remodeling, and caused an on-going angiogenesis [20]. In the present study, sorafenib exhibited an inhibitory trend on pulmonary VEGFR-2 and VEGF-A transcripts, and caused a significant suppression on

VEGF-A protein level, which were consistent with the results by Moreno-Vinasco et al. [30]. However, an escape angiogenesis [3] did not occur in these groups. Instead, all of the sorafenib groups showed significant ERK 1/2 de-phosphorylation and low nestin mRNA levels. This was further evident by the concurrent low level of the CXCR4 mRNA, a vascular marker for vessel sprouting [35,36] and the main inducer of vasculogenesis [1] in the sorafenib groups. We speculate that sorafenib preserves its potent anti-remodeling property via direct Raf-1 inhibition which cuts the entry signal [4] from the VEGFR-2 to the downstream MAPK pathway [13]. On the contrary, the potent VEGFR-2 inhibitor toceranib surprisingly did not significantly reduce pulmonary VEGFR-2 mRNA nor protein levels, and only the highest dose significantly suppressed VEGF-A protein expression. We also observed no significant nestin nor CXCR4 mRNA upregulation in the toceranib groups to indicate small vessel proliferation [27,32,33] or sprouting [35,36] in the lungs. Taken together, these results suggest that the weak reversal effects of toceranib on pulmonary remodeling may not be due to VEGF signaling inhibition.

Because the lowest sorafenib dose and the highest toceranib dose yielded comparable phosphorylated ERK protein levels, we speculated that the stronger reversal effects by sorafenib compared with toceranib might be also governed by other mechanisms or pathways, in addition to the MAPK pathway. Long et al. [26] showed that rats treated for 3 weeks with MCT had an increased LC3B-II level in the small pulmonary arterial walls and a decreased p-62 staining in the medial layer of FMPAs. However, a recent study of Sugen/hypoxia-induced PAH by Kato et al. [12] revealed that the autophagy in endothelial cells was time-dependent, in which the LC3 level decreased by 3 weeks after an initial increase, and rapamycin as an autophagy activator ameliorated PAH and CPR. Consistent with the above finding, we showed that the MCT-treated rats did not upregulate the LC3-

II protein nor p-62 transcript levels, suggesting the presence of apoptosis-resistant cells [12] at 4 weeks after the MCT injection. In the treatment groups, sorafenib but not toceranib increased the LC3-II protein and p-62 mRNA expression, implying an autophagy induction in the lungs by sorafenib, probably via inhibition on the PI3K/AKT/mTOR signaling pathway [21,40]. Furthermore, while Lin et al. [21,22] showed that sorafenib influenced interleukin secretion and function of dendritic cells and macrophages, several studies reported that the CXCL12/CXCR4 inhibition improved hypoxia-induced PAH [6,7,39]. The present study is the first to document that the MCT treatment upregulated the CXCL12/CXCR4 transcript levels, suggesting a pathogenic role of this pathway in the MCT-induced PAH. With respect to this, since the CXCR4 mRNA downregulation was greater in sorafenib than in toceranib, we speculate that sorafenib may also ameliorate PAH by blocking the CXCR4/SDF-1 signaling which further suppressed recruitment of PDGF and c-KIT receptors in the lungs [41].

The present study has some limitations as we did not evaluate the PI3K/AKT/mTOR and adenosine monophosphate-activated protein kinase (AMPK) signaling pathways which may further elucidate the reversal differences between sorafenib and toceranib. However, the above results led us to believe that sorafenib strongly reversed PAH and CPR by not only mainly blocking the MAPK, but also the CXCL12/CXCR4 signaling, and inducing autophagy in the apoptosis-resistant pulmonary tissues.

5. Conclusion

Toceranib showed weaker reversal effects on cardiopulmonary remodeling and RV hemodynamic improvement compared with sorafenib. A high dose (10 mg/kg) of toceranib partially ameliorated pulmonary arterial muscularization but did not improve PAH, precluding the use of toceranib in the treatment of PAH. On the contrary, despite

the stronger VEGF inhibitory activity in the lungs, sorafenib did not exaggerate but significantly and dose-dependently reversed cardiopulmonary remodeling and PAH at even a low dose (10 mg/kg). This may be due to the concurrent potent inhibition on Raf-1 kinase and CXCR4, and possibly the autophagy-inducing property of sorafenib, which made a low dose suitable for the treatment of PAH.

Acknowledgements

We thank Prof. Dr. Yoshiaki Yamano, Prof. Dr. Takehito Morita, Dr. Masahi Higuchi, Dr. Naoki Kitamura and Dr. Sae Sanematsu for their valuable technical assistance.

Declaration of interest

This study was supported in part by the Grant-in-Aid for challenging Exploratory Research (no. 25660240; to Y. Hikasa) and for Scientific Research (C) (no. 18K05993; to Y. Hikasa) from the Japan Society for the Promotion of Science.

Figure captions

Fig. 1. Effects of sorafenib and toceranib on right ventricular systolic pressure (RVSP), mean right ventricular pressure (RVP) and heart rate (n=4–6) (A), right ventricular hypertrophy (RVH) and dose-dependent reversal (n=8–14) (B), and b-type natriuretic peptide messenger RNA (mRNA) expression normalized to glyceraldehyde-3-phosphate dehydrogenase (GAPDH) of the right ventricle tissue (n=8–14) (C). Data are means±standard error of mean (SEM). *P<0.05 versus control, †P<0.05 versus placebo.

Fig. 2. Effects of sorafenib and toceranib on vascular muscularization in 20–50-μm intra-acinar arteries. Photomicrographs represent intra-acinar pulmonary arteries that are (i) non-muscularized (NMPA), (ii) partially muscularized (PMPA), and (iii) fully muscularized (FMPA) (A). Proportion of each artery type related to the total number of pulmonary arteries (B) and dose-dependent reversal of sorafenib and toceranib on FMPAs (C) and NMPAs (D) are shown. Data are means±SEM (n=8–12). *P<0.05 versus control, †P<0.05 versus placebo.

Fig. 3. Effects of sorafenib and toceranib on medial wall thickness normalized to the external diameter (A,C) and lumen area (B,D) of the 20–50 μm (A,B) and 51–100 μm (C,D) FMPAs, respectively. Data are means±SEM (n=8–12). *P<0.05 versus control, †P<0.05 versus placebo.

Fig. 4. Effects of sorafenib and toceranib on monocrotaline-induced mRNA expression of platelet-derived growth factor receptor-β (PDGFR-β) (n=8–14) (A), KIT proto-oncogene receptor tyrosine kinase (c-KIT) (n=8–10) (B), C-X-C chemokine receptor type 4 (CXCR4) (n=8–11) and ligand 12 (CXCL12) (n=8–12) (C) in rat lungs. Data are means±SEM. *P<0.05 vs control, †P< 0.05 vs placebo.

Fig. 5. Effects of sorafenib and toceranib on monocrotaline-induced vascular endothelial

growth factor (VEGF) signaling pathway (A,B,C) and nestin mRNA expression (n=8–14) (D) in rat lungs. The VEGF signaling pathway is represented by VEGF receptor-2 (VEGFR-2) mRNA (n=8–12) and protein expression (n= 4–5) (A), and VEGF-A mRNA (n=7–9) and protein expression (n=3–4) (C). Western blots represent VEGFR-2 and VEGFR-A protein expression of one individual from each group (B). Data are means ± SEM. *P<0.05 versus control, †P<0.05 versus placebo.

Fig. 6. Effects of sorafenib and toceranib on mitogen-activated protein kinase signaling in rat lungs, indicated by Raf-1 proto-oncogene serine/threonine kinase (Raf-1) mRNA expression (n=8–14) (A) and extracellular-signal-related kinase (ERK)-1/2 protein phosphorylation (C). Western blots represent phosphorylated versus total ERK protein of one individual from each group (n=3–4) (B). Data are means±SEM. *P<0.05 versus control, †P<0.05 versus placebo.

Fig. 7. Effects of sorafenib and toceranib on expression of microtubule-associated protein 1 light chain (LC) 3-II protein normalized to β-actin (n=5–6) (A), and p-62 mRNA (n=8–17) (B). Western blots represent LC3-II protein expression of one individual from each group (A). Data are means±SEM. *P<0.05 versus control, †P<0.05 versus placebo.

References

[1] Aghi M, Cohen KS, Klein RJ, Scadden DT, Chiocca EA. Tumor stromal-derived factor-1 recruits vascular progenitors to mitotic neovasculature, where microenvironment influences their differentiated phenotypes. *Cancer Res* 2006; **66**: 9054–9064.

[2] Arita S, Arita N, Hikasa Y. Therapeutic effect of low-dose imatinib on pulmonary arterial hypertension in dogs. *Can Vet J* 2013; **54**: 255–261.

[3] Carmeliete PK. Keystone Conference of Pulmonary Hypertension. September 10-15, 2012. Monterey, California USA. [Personal communication]

[4] Dhillon AS, Kolch W. Untying the regulation of the Raf-1 kinase. *Arch Biochem Biophys* 2002; **404**: 3–9.

[5] Farber HW, Miller DP, Poms AD, Badesch DB, Frost AE, Muros-Le Rouzic E, et al. Five-year outcomes of patients enrolled in the REVEAL registry. *Chest* 2015; **148**:1043–1054.

[6] Farkas D, Kraskauskas D, Drake JI, Alhussaini AA, Kraskauskiene V, Bogaard HJ, et al. CXCR4 inhibition ameliorates severe obliterative pulmonary hypertension and accumulation of C-kit$^+$ cells in rats. *PLoS One* 2014; **9**: e89810.

[7] Gambaryan N, Perros F, Montani D, Cohen-Kaminsky S, Mazmanian M, Renaud JF, et al. Targeting of c-kit+ haematopoietic progenitor cells prevents hypoxic pulmonary hypertension. *Eur Respir J* 2011; **37**: 1392–1399.

[8] Ghofrani HA, Morrell NW, Hoeper MM, Olschewski H, Peacock AJ, Barst RJ, et al. Imatinib in pulmonary arterial hypertension patients with inadequate response to established therapy. *Am J Respir Crit Care Med* 2010; **182**: 1171–1177.

[9] Gómez-Sánchez R, Yakhine-Diop SM, Rodríguez-Arribas M, Bravo-San Pedro JM, Martínez-Chacón G, Uribe-Carretero E. mRNA and protein dataset of autophagy markers (LC3 and p62) in several cell lines. *Data Brief* 2016; **7**: 641–647.

[10] Hatano M, Yao A, Shiga T, Kinugawa K, Hirata Y, Nagai R. Imatinib mesylate has the potential to exert its efficacy by down-regulating the plasma concentration of platelet-derived growth factor in patients with pulmonary arterial hypertension. *Int Heart J* 2010; **51**: 272–276.

[11] Hoeper MM, Barst RJ, Bourge RC, Feldman J, Frost AE, Galie N, et al. Imatinib mesylate as add-on therapy for pulmonary arterial hypertension: Results of the randomized IMPRES study. *Circulation* 2013; **127**: 1128–1138.

[12] Kato F, Sakao S, Takeuchi T, Suzuki T, Nishimura R, Yasuda T, at al. Endothelial cell-related autophagic pathways in Sugen/hypoxia-exposed pulmonary arterial hypertensive rats. *Am J Physiol Lung Cell Mol Physiol* 2017; **313**: L899–L915.

[13] Katz M, Amit I, Yarden Y. Regulation of MAPKs by growth factors and receptor tyrosine kinases. *Arch Biochem Biophys* 2007; **1773**: 1161–1176.

[14] Kimura G, Kataoka M, Inami T, Fukuda K, Yoshino H, Satoh T. Sorafenib as a potential strategy for refractory pulmonary arterial hypertension. *Pulm Pharmacol Ther* 2017; **44**: 46–49.

[15] Kitagawa D, Yokota K, Gouda M, Narumi Y, Ohmoto H, Nishiwaki E, et al. Activity-based kinase profiling of approved tyrosine kinase inhibitors. *Genes Cells* 2013; **18**: 110–122.

[16] Klein M, Schermuly RT, Ellinghaus P, Milting H, Riedl B, Nikolova S, et al. Combined tyrosine and serine/threonine kinase inhibition by sorafenib prevents

progression of experimental pulmonary hypertension and myocardial remodeling. *Circulation* 2008; **118**: 2081–2090.

[17] Kojonazarov B, Sydykov A, Pullamsetti SS, Luitel H, Dahal BK, Kosanovic D, et al. Effects of multikinase inhibitors on pressure overloaded-induced right ventricular remodeling. *Int J Cardiol* 2013; **167**: 2630–2637.

[18] Leblanc AK, Miller AN, Galyon GD, Moyers TD, Long MJ, Stuckey AC, et al. Preliminary evaluation of serial (18) FDG-PET/CT to assess response to toceranib phosphate therapy in canine cancer. *Vet Radiol Ultrasound* 2012; **53**: 348–357.

[19] Lee SJ, Smith A, Guo L, Alastalo TP, Li M, Sawada H, et al. Autophagic protein LC3B confers resistance against hypoxia-induced pulmonary hypertension. *Am J Respir Crit Care Med* 2011; **183**: 649–658.

[20] Leong ZP, Okida A, Higuchi M, Yamano Y, Hikasa Y. Reversal effects of low-dose imatinib compared with sunitinib on monocrotaline-induced pulmonary and right ventricular remodeling in rats. *Vascul Pharmacol* 2018; **100**: 41–50.

[21] Lin JC, Huang WP, Liu CL, Lee JJ, Liu TP, Ko WC, et al. Sorafenib induces autophagy in human myeloid dendritic cells and prolongs survival of skin allografts. *Transplantation* 2013; **95**: 791–800.

[22] Lin JC, Liu CL, Lee JJ, Liu TP, Ko WC, Huang WC, et al. Sorafenib induces autophagy and suppresses activation of human macrophage. *Int Immunopharmacol* 2013; **15**: 333-339.

[23] London C, Mathie T, Stingle N, Clifford C, Haney S, Klein MK, et al. Preliminary evidence for biologic activity of toceranib phosphate (Palladia(®)) in solid tumours. *Vet Comp Oncol* 2012; **10**: 194–205.

[24] London CA, Hannah AL, Zadovoskaya R, Chien MB, Kollias-Baker C, Rosenberg M, et al. Phase I dose-escalating study of SU11654, a small molecule receptor tyrosine kinase inhibitor, in dogs with spontaneous malignancies. *Clin Cancer Res* 2003; **9**: 2755–2768.

[25] London CA, Malpas PB, Wood-Follis SL, Boucher JF, Rusk AW, Rosenberg MP, et al. Multi-center, placebo-controlled, double-blind, randomized study of oral toceranib phosphate (SU11654), a receptor tyrosine kinase inhibitor, for the treatment of dogs with recurrent (either local or distant) mast cell tumor following surgical excision. *Clin Cancer Res* 2009; **15**: 3856–3865.

[26] Long L, Yang X, Southwood M, Lu J, Marciniak SJ, Dunmore BJ, et al. Chloroquine prevents progression of experimental pulmonary hypertension via inhibition of autophagy and lysosomal bone morphogenetic protein type II receptor degradation. *Circ Res* 2013; **112**: 1159–1170.

[27] Matsuda Y, Hagio M, Ishiwata T. Nestin: A novel angiogenesis marker and possible target for tumor angiogenesis. *World J Gastroenterol* 2013; **19**: 42–48.

[28] Minami H, Kawada K, Ebi H, Kitagawa K, Kim YI, Araki K, et al. Phase I and pharmacokinetic study of sorafenib, an oral multikinase inhibitor, in Japanese patients with advanced refractory solid tumors. *Cancer Sci*. 2008; **99**:1492–1498.

[29] Montani D, Chaumais M-C, Guignabert C, Gunther S, Girerd B, Jais X, et al. Targeted therapies in pulmonary arterial hypertension. *Pharmacol Ther* 2014; **141**: 172–191.

[30] Moreno-Vinasco L, Gomberg-Maitland M, Maitland ML, Desai AA, Singleton PA, Sammani S, et al. Genomic assessment of a multikinase inhibitor, sorafenib,

in a rodent model of pulmonary hypertension. *Physiol Genomics* 2008; **33**: 278–291.

[31] Nicolls M, Mizuno S, Taraseviciene-Stewart L, Farkas L, Drake JI, Husseini AA, et al. New models of pulmonary hypertension based on VEGF receptor blockade-induced endothelial cell apoptosis. *Pulm Circ* 2012; **2**: 434–442.

[32] Oikawa H, Hayashi K, Maesawa C, Masuda T, Sobue K. Expression profiles of nestin in vascular smooth muscle cells in vivo and in vitro. *Exp Cell Res* 2010; **316**: 940–950.

[33] Saboor F, Reckmann AN, Tomczyk CU, Peters DM, Weissmann N, Kaschtanow A, et al. Nestin-expressing vascular wall cells drive development of pulmonary hypertension. *Eur Respir J* 2016; **47**: 876–888.

[34] Schermuly RT, Dony E, Ghofrani HA, Pullamsetti S, Savai R, Roth M, et al. Reversal of experimental pulmonary hypertension by PDGF inhibition. *J Clin Invest* 2005; **115**: 2811–2821.

[35] Strasser GA, Kaminker JS, Tessier-Lavigne M. Microarray analysis of retinal endothelial tip cells identifies CXCR4 as a mediator of tip cell morphology and branching. *Blood* 2010; 115: 5102–5110.

[36] Xu J, Liang J, Meng YM, Yan J, Yu XJ, Liu CQ, et al. Vascular CXCR4 expression promotes vessel sprouting and sensitivity to sorafenib treatment in hepatocellular carcinoma. Clin Cancer Res 2017; **23**: 4482–4492.

[37] Yancey MF, Merritt DA, Lesman SP, Boucher JF, Michels GM. Pharmacokinetic properties of toceranib phosphate (Palladia, SU11654), a novel tyrosine kinase inhibitor, in laboratory dogs and dogs with mast cell tumors. *J Vet Pharmacol Ther*. 2010; **33**:162–171.

[38] Yoshii SR, Mizushima N. Monitoring and measuring autophagy. *Int J Mol Sci* 2017; **18**, 1865.

[39] Young KC, Torres E, Hatzistergos KE, Hehre D, Suguihara C, Hare JM. Inhibition of the SDF-1/CXCR4 axis attenuates neonatal hypoxia-induced pulmonary hypertension. *Circ Res* 2009; **104**: 1293–1301.

[40] Zhang CZ, Wang XD, Wang HW, Cai Y, Chao LQ. Sorafenib inhibits liver cancer growth by decreasing mTOR, AKT, and PI3K expression. *J BUON* 2015; **20**: 218–222.

[41] Zernecke A, Schober A, Bot I, von Hundelshausen P, Liehn EA, Möpps B, et al. SDF-1alpha/CXCR axis is instrumental in neointimal hyperplasia and recruitment of smooth muscle progenitor cells. *Circ Res* 2005; **96**: 784–791.

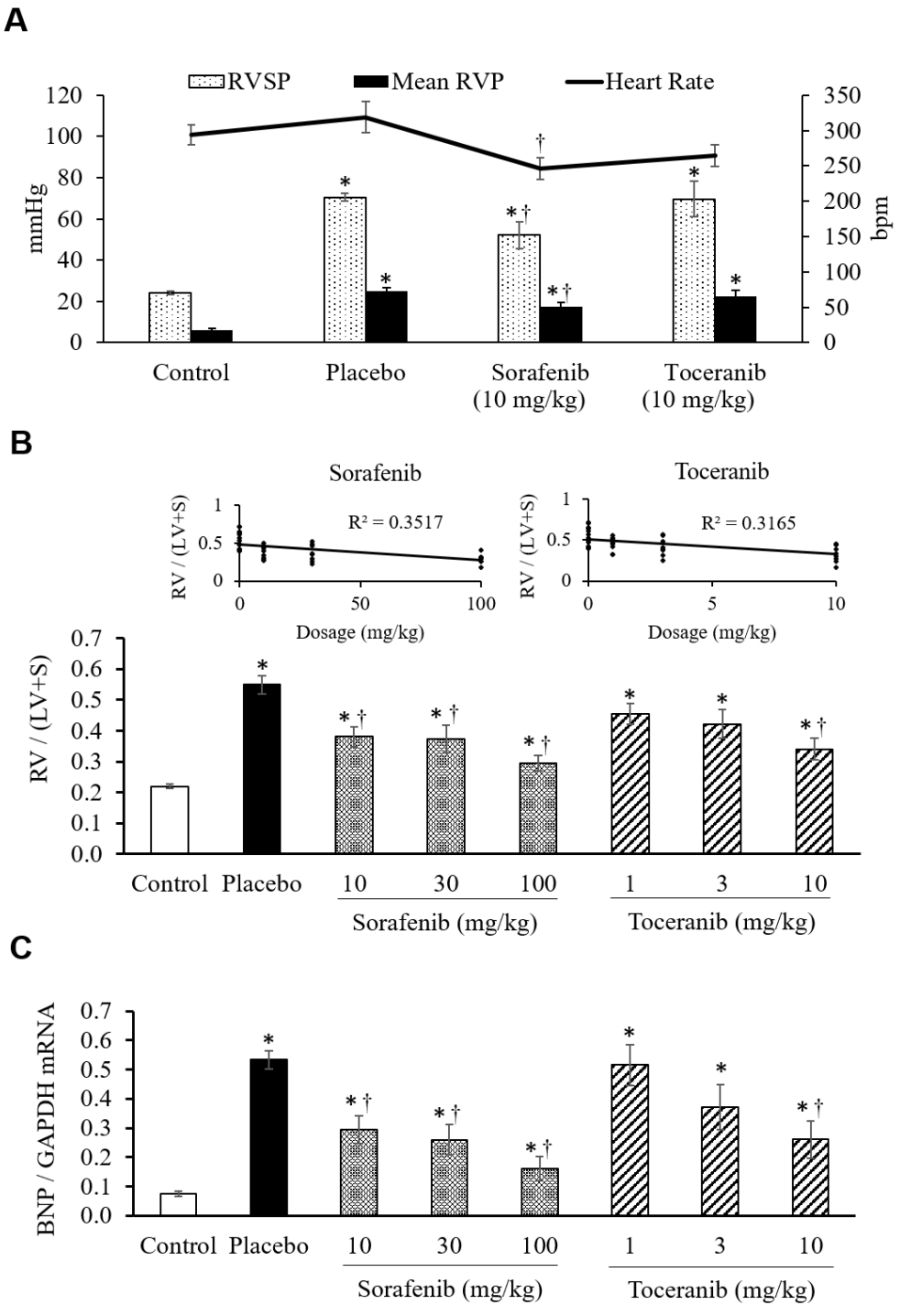
A
RVSP
Mean RVP
Heart Rate
mmHg
bpm
Control
Placebo
Sorafenib (10 mg/kg)
Toceranib (10 mg/kg)
B
Sorafenib
Toceranib
R² = 0.3517
R² = 0.3165
RV / (LV+S)
Dosage (mg/kg)
Control
Placebo
Sorafenib (mg/kg)
Toceranib (mg/kg)
C
BNP / GAPDH mRNA

Figure 1

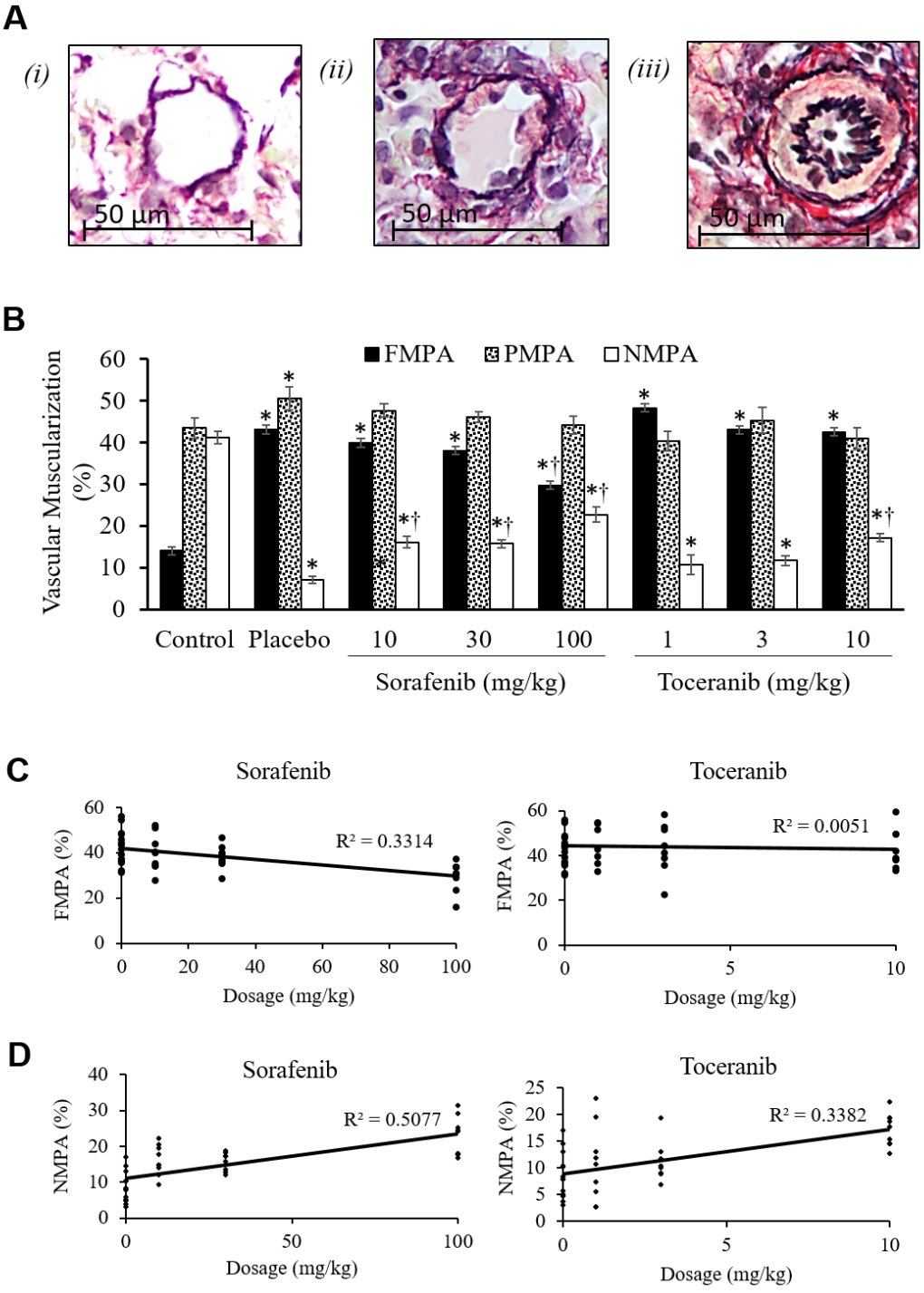
A
(i)
50 µm
(ii)
50 µm
(iii)
50 µm
B
FMPA
PMPA
NMPA
Vascular Muscularization (%)
60
50
40
30
20
10
0
Control
Placebo
10
30
100
1
3
10
Sorafenib (mg/kg)
Toceranib (mg/kg)
C
Sorafenib
R² = 0.3314
FMPA (%)
Dosage (mg/kg)
Toceranib
R² = 0.0051
FMPA (%)
Dosage (mg/kg)
D
Sorafenib
R² = 0.5077
NMPA (%)
Dosage (mg/kg)
Toceranib
R² = 0.3382
NMPA (%)
Dosage (mg/kg)

Figure 2

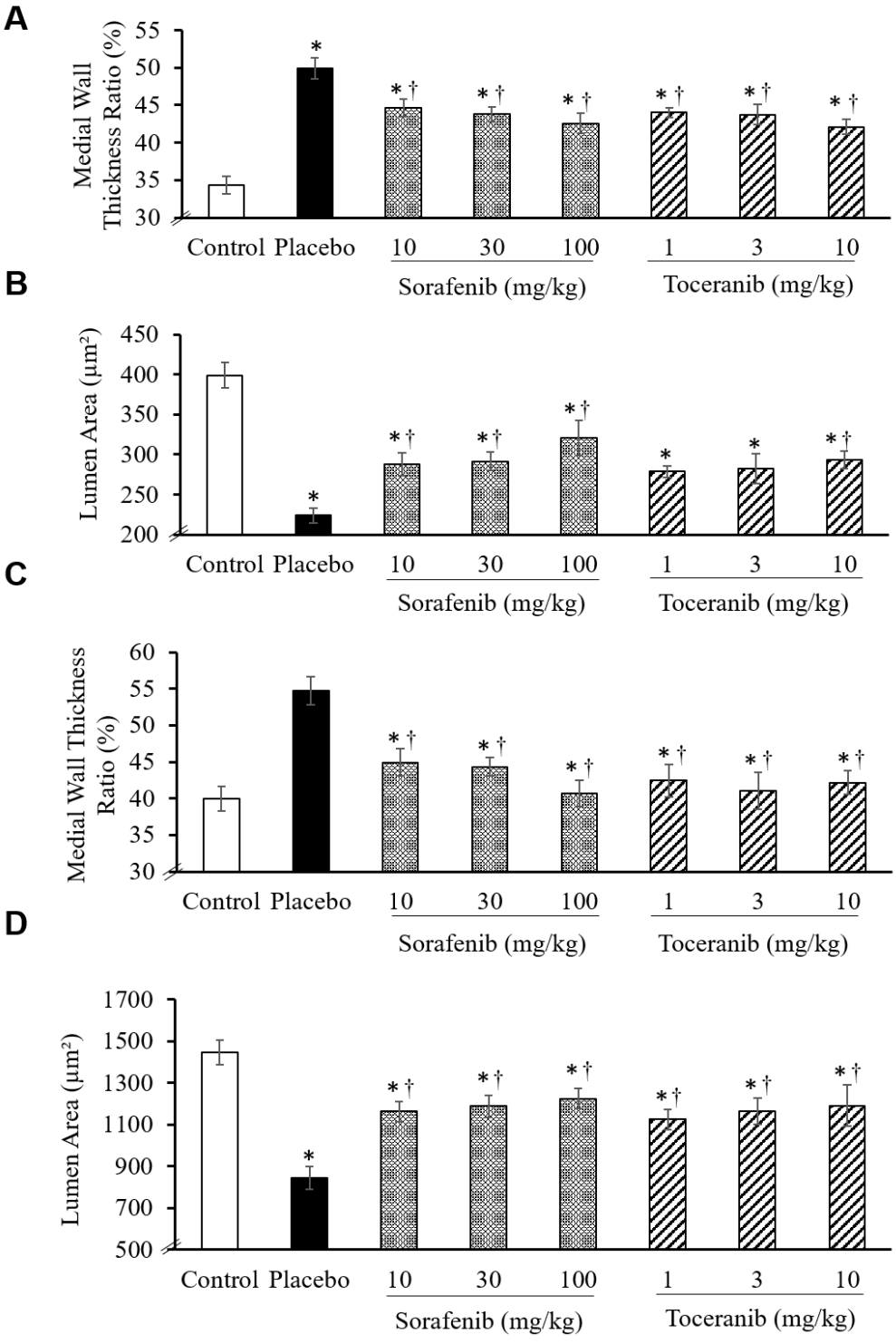
A
Medial Wall Thickness Ratio (%)
55
50
45
40
35
30
Control Placebo
10
30
100
1
3
10
Sorafenib (mg/kg)
Toceranib (mg/kg)
B
Lumen Area (μm²)
450
400
350
300
250
200
Control Placebo
10
30
100
1
3
10
Sorafenib (mg/kg)
Toceranib (mg/kg)
C
Medial Wall Thickness Ratio (%)
60
55
50
45
40
35
30
Control Placebo
10
30
100
1
3
10
Sorafenib (mg/kg)
Toceranib (mg/kg)
D
Lumen Area (μm²)
1700
1500
1300
1100
900
700
500
Control Placebo
10
30
100
1
3
10
Sorafenib (mg/kg)
Toceranib (mg/kg)

Figure 3

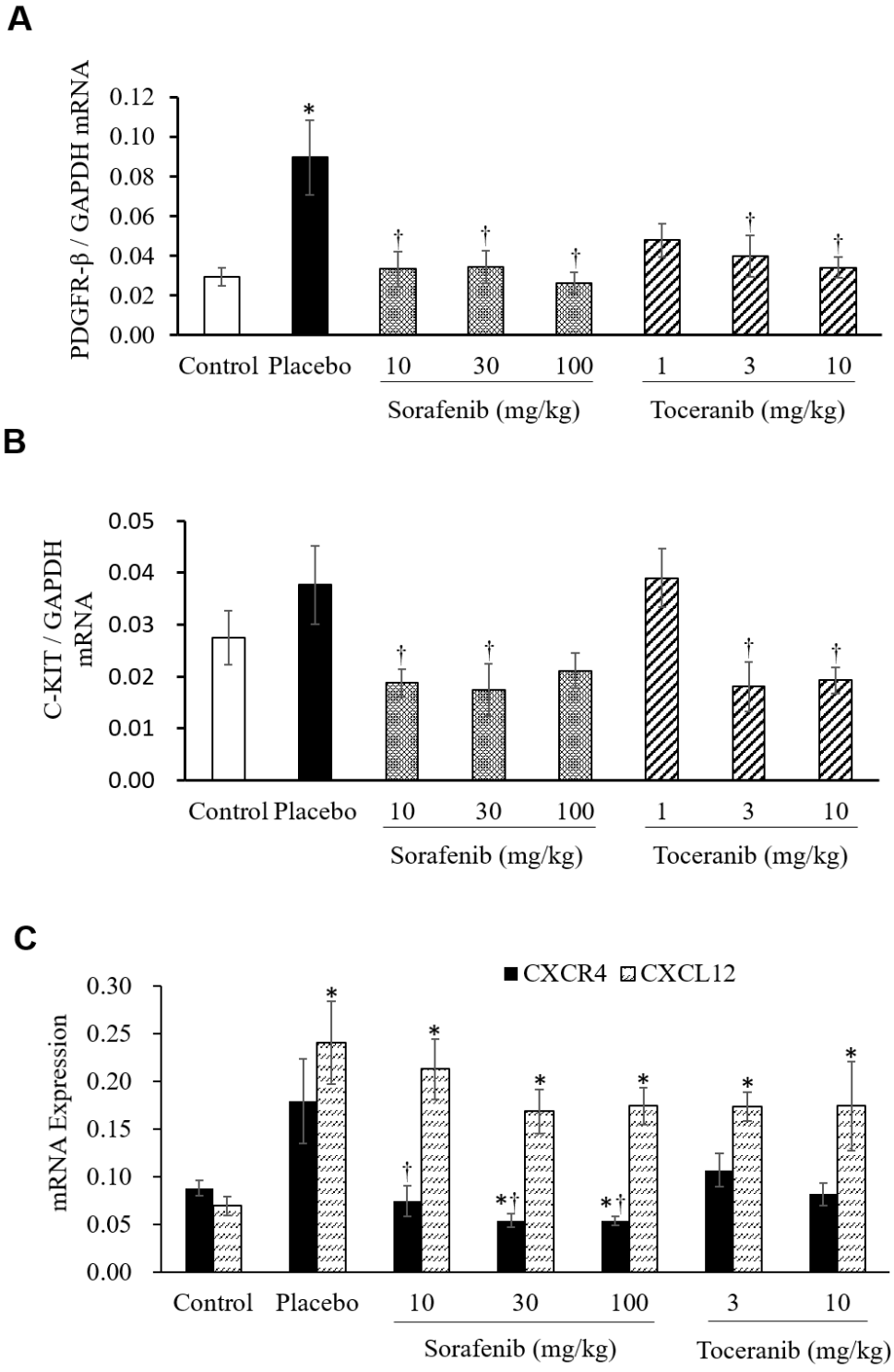
A
PDGFR-β / GAPDH mRNA
0.12
0.10
0.08
0.06
0.04
0.02
0.00
Control Placebo 10 30 100 1 3 10
Sorafenib (mg/kg)
Toceranib (mg/kg)
B
C-KIT / GAPDH mRNA
0.05
0.04
0.03
0.02
0.01
0.00
Control Placebo 10 30 100 1 3 10
Sorafenib (mg/kg)
Toceranib (mg/kg)
C
CXCR4 CXCL12
mRNA Expression
0.30
0.25
0.20
0.15
0.10
0.05
0.00
Control Placebo 10 30 100 3 10
Sorafenib (mg/kg)
Toceranib (mg/kg)

Figure 4

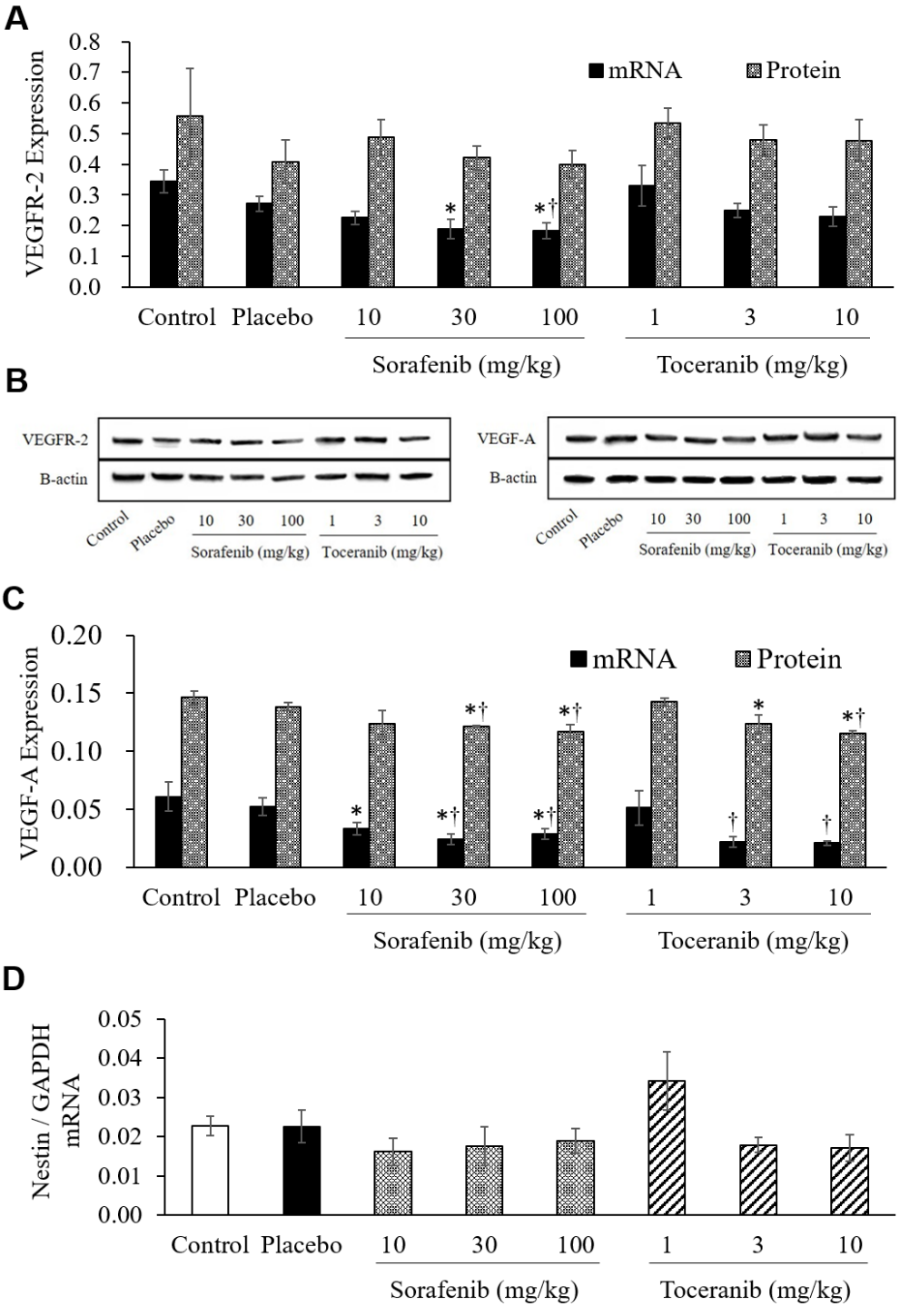
A
VEGFR-2 Expression
0.8
0.7
0.6
0.5
0.4
0.3
0.2
0.1
0.0
mRNA
Protein
*
*†
Control
Placebo
10
30
100
1
3
10
Sorafenib (mg/kg)
Toceranib (mg/kg)
B
VEGFR-2
B-actin
VEGF-A
B-actin
Control
Placebo
10
30
100
1
3
10
Sorafenib (mg/kg)
Toceranib (mg/kg)
C
VEGF-A Expression
0.20
0.15
0.10
0.05
0.00
mRNA
Protein
*
*†
†
Control
Placebo
10
30
100
1
3
10
Sorafenib (mg/kg)
Toceranib (mg/kg)
D
Nestin / GAPDH mRNA
0.05
0.04
0.03
0.02
0.01
0.00
Control
Placebo
10
30
100
1
3
10
Sorafenib (mg/kg)
Toceranib (mg/kg)

Figure 5

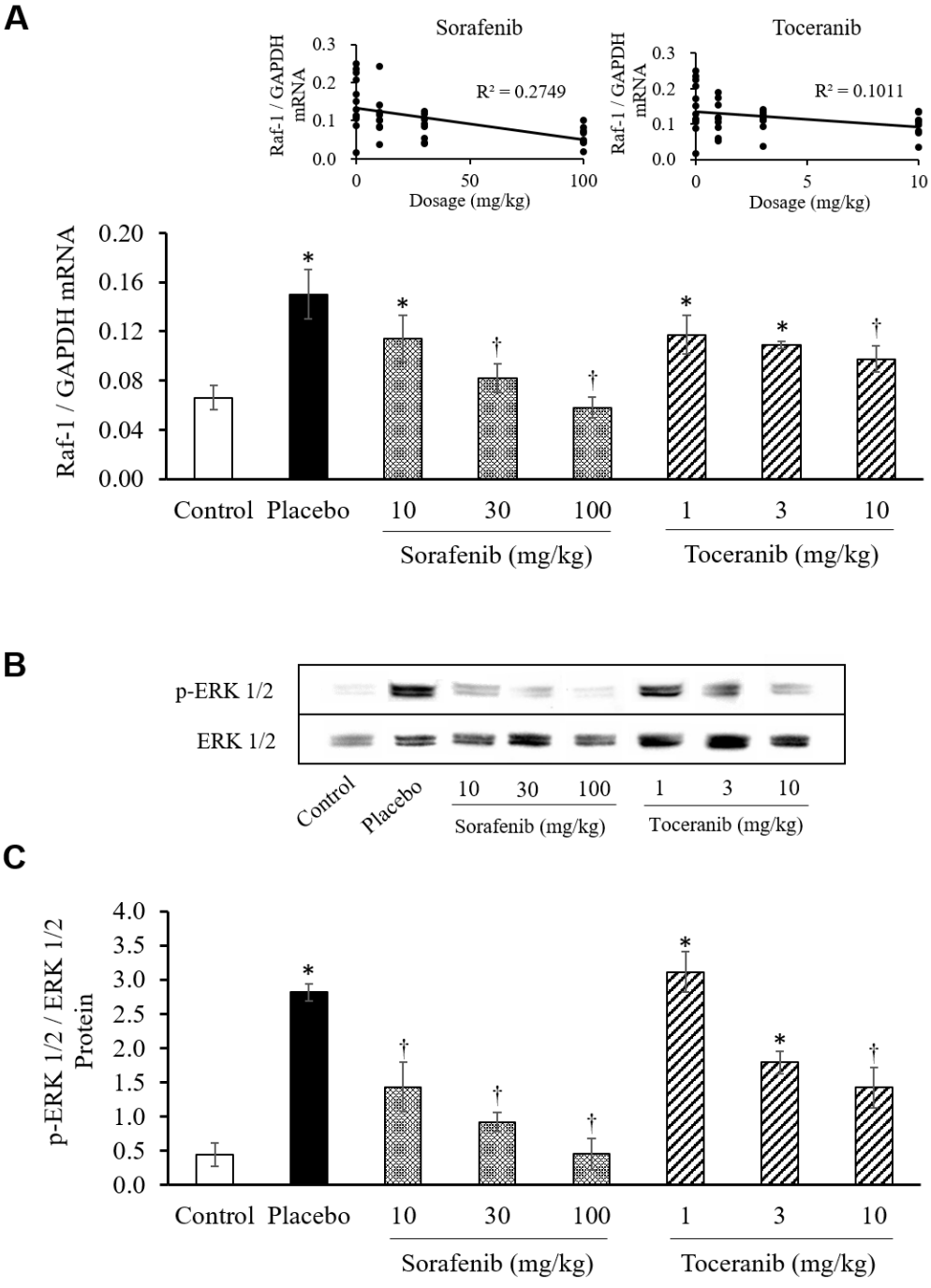
A
Sorafenib
Toceranib
Raf-1 / GAPDH mRNA
R² = 0.2749
R² = 0.1011
Dosage (mg/kg)
Raf-1 / GAPDH mRNA
Control
Placebo
10
30
100
1
3
10
Sorafenib (mg/kg)
Toceranib (mg/kg)
B
p-ERK 1/2
ERK 1/2
C
p-ERK 1/2 / ERK 1/2 Protein

Figure 6

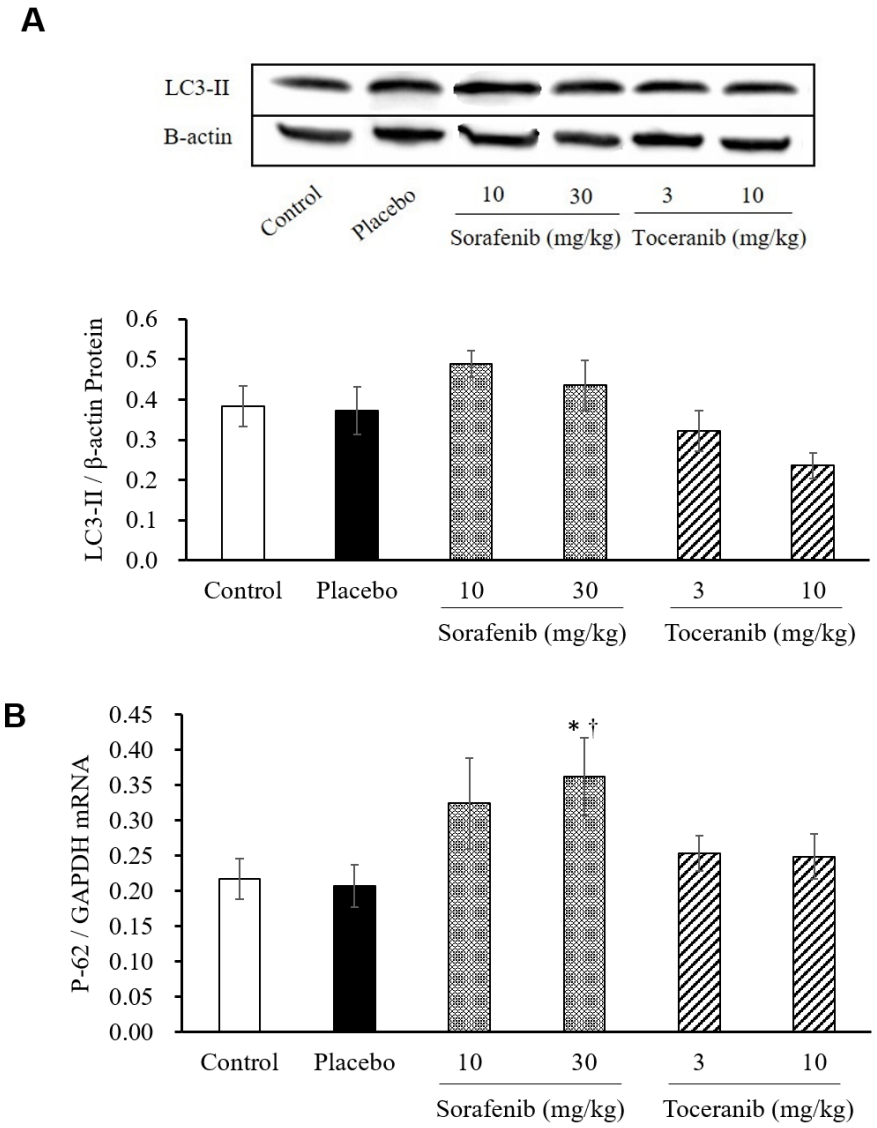
A
LC3-II
B-actin
Control
Placebo
10
30
3
10
Sorafenib (mg/kg)
Toceranib (mg/kg)
LC3-II / β-actin Protein
0.6
0.5
0.4
0.3
0.2
0.1
0.0
Control
Placebo
10
30
3
10
Sorafenib (mg/kg)
Toceranib (mg/kg)
B
P-62 / GAPDH mRNA
0.45
0.40
0.35
0.30
0.25
0.20
0.15
0.10
0.05
0.00
* †
Control
Placebo
10
30
3
10
Sorafenib (mg/kg)
Toceranib (mg/kg)

Figure 7